

Accounting for multiplicity in machine learning benchmark performance

Kajsa Møllersen¹ and Einar Holsbø²

¹Department of Community Medicine

²Department of Computer Science
UiT - The Arctic University of Norway

1 Estimating state-of-the-art performance

In this article, we direct attention to the reporting of state-of-the-art classifier performance by presenting the sample maximum estimator distribution function and analysing its bias. This analysis is done using the framework of multiplicity.

Within the fields of research that develop, refine, test and use classifiers, the term state-of-the-art (SOTA) commonly refers to the highest reported performance to date, and is used as a reference point when presenting and comparing models. The reported performance of a classifier, originating from applying that classifier to a specific data set, a sample, is in effect an estimate of that classifier's underlying population performance.

The highest reported performance among a number of classifiers serves as an estimate of SOTA, although the term 'estimate' is seldom used explicitly in the SOTA context. The highest reported performance corresponds to the sample maximum of population performances, and this estimator is biased when used to estimate SOTA. The sample maximum gives in overoptimistic estimates of the maximum population performance, and is problematic as a reference point in research. The mechanisms creating this bias comes from multiplicity, and the fact that the we pick the highest sample performance among multiple classifier results.

In its simplest form, with independent binary classifiers with identical probability of success, the distribution function of the sample maximum estimator exists in closed form with only a few parameters, and can be directly applied to calculate and analyse the bias in a certain situation. With growing complexity, such as mutual dependencies and more elaborate performance measures, the distribution function of the estimator is no longer known, but the mechanisms at play and the pitfalls to be aware of are much the same, and limited studies can be done by straightforward simulations.

Machine learning models are commonly evaluated and compared by their performance on data sets from public repositories, where models can be eval-

uated under identical conditions and across time. Theoretical results play an important role in machine learning research, but for the last couple of decades the success of increasingly complex models has pushed the proof towards the pudding: performance on benchmark data sets.

The numbers don't lie: if model A performs better than model B on a specific data set, that is what it did. But the truth that these numbers tell is limited. We are interested in the population performance, and the sample performance is only an estimate. A good estimating procedure gives a reliable result, and there are plenty of pitfalls to be aware of: Overfitting to the data set, originating from wrong use of cross-validation, data leakage and data reuse, can give overly optimistic estimates. An independent test set, often referred to as a hold-out set, is a sample that is not used for development of the model, and prevents overfitting. Competitions and challenges with prize money typically withhold the test set so that it becomes impossible for the participants to use it for training.

The highest ranked performance on a problem is referred to as SOTA performance, and is used, among other things, as a reference point for publication of new models. As a specific model's performance on a test set is just an estimate of its true underlying performance, the reported SOTA performances are estimates, and hence come with bias and variance. The practice of hold-out test sets in competitions safe-guards against overoptimistic estimates for the individual classifiers. Data is often released after the competition has ended, and new methods can be compared to the SOTA performance.

As we will show in the subsequent sections, using the highest-ranked performance as an estimate for SOTA is a biased estimator, giving overoptimistic results. The mechanisms at play are those of multiplicity, a topic that is well-studied in the context of multiple comparisons and multiple testing, but has, as far as the authors are aware of, been nearly absent from the discussion regarding SOTA estimates.

Biased SOTA estimation has consequences both for practical implementations and for research itself. A health care provider might want to use some machine learning method for tumour detection, but only if the method correctly classifies at least 80%. They follow updates on SOTA performance, and are ready to invest time and money in a pilot project once the lower bound surpasses 80%. If the SOTA performance is an optimistic estimate, the health care provider has now lost time and money, and perhaps also some faith in research results.

For the research community, the situation is perhaps even more dramatic. The optimistic SOTA estimate is used as a standard for evaluating new methods. Not to say that a new method necessarily needs to beat the current SOTA to catch interest from reviewers and editors, but it certainly helps if its performance is comparable. It has been pointed out (see Section 2) that the incremental increase in performance can obstruct the spread of new ideas that have substantial potential, but just haven't reached their peak yet.

In this article, we provide a probability distribution for the case of multiple classifiers. We demonstrate the impact of multiplicity through simulated exam-

ples. We show how classifier dependency impacts the variance, but also that the impact is limited when the probability of success is high. Finally, we discuss three real-world examples that each highlights different aspects multiplicity and SOTA estimation. All code is available at <https://github.com/3inar/ninety-nine>.

2 Related work

Multiple comparisons is a well-studied subject within statistics, see, e.g., Tukey [1991] for an interesting discussion on some topics of multiple comparisons, among them the confidence intervals (CIs). For a direct demonstration of how multiple testing can lead to false discoveries, Bennett et al. [2009] give an example where brain activity is detected in (dead) salmon “looking” at photos of people. In the machine learning context, with multiple data sets and classifiers, Demšar [2006] suggests adjusting for multiple testing, according to well-known statistical theory. Our article focuses on the estimate itself and its uncertainty, and not comparison of methods.

The re-use of benchmark datasets has been addressed in several publications. Salzberg [1997] point to the problem that arises because these datasets are static, and therefore run the risk of being exhausted by overfitting. Exhausted public data sets still serve important functions, e.g., a new idea can show to perform satisfactory, even when it is not superior. Thompson et al. [2020] distinguish between simultaneous and sequential multiple correction procedures. In sequential testing, which is the reality of public datasets, the number of tests is constantly updated. An interesting topic they bring up is the conflict between sharing incentive, open access and stable false positive rate. There are several demonstrations of the vulnerability of re-use of benchmark datasets. Teney et al. [2020] performed a successful attack on the VQA-CP benchmark dataset, that is, they are able to attain high performance with a non-generalisable classifier. They point towards the risk of ML methods capturing idiosyncrasies of a dataset. Torralba and Efros [2011] introduced the game Name That Dataset! motivating their concern of methods being tailored to a dataset rather than a problem. The lack of statistically significant differences among top performing methods is demonstrated by, e.g., Everingham et al. [2015] and Fernández-Delgado et al. [2014].

The same mechanisms of overfitting are present in challenges through multiple submissions to the validation set. Blum and Hardt [2015] introduced an algorithm that releases the public leaderboard score only if there has been significant improvement compared to the previous submission. This will prevent overfitting by hindering adjustments to random fluctuations in the score and not true improvements of the method. Dwork et al. [2017] used the principles of differential privacy to prevent overfitting to the validation set.

Several publications show that the overfitting is not as bad as expected, and provide possible explanations. Recht et al. [2019] constructed new, independent test sets of CIFAR-10 and ImageNet. They found that the accuracy drop is

dramatic, around 10%. However, the order of the best performing methods is preserved, which can be explained by the fact that multiple classes (Feldman et al. [2019]) and model similarity (Mania et al. [2019]) slow down overfitting. Roelofs et al. [2019] compared the results from the private leaderboard (one submission per team) and the public leaderboard (several submissions per team) in Kaggle challenges. Several of their analyses indicate overfitting even though their main conclusion is that there is little evidence of overfitting.

Overfitting and its consequences are avoided in most challenges by withholding the test set so that a method can only be evaluated once and not adapted to the test set performance. Hold-out datasets also prevents wrong use of cross-validation, see, e.g., Fernández-Delgado et al. [2014] and the seminal paper of Dietterich [1998]. Another contribution from public challenges is the requirement of reproducibility to collect the prize money, which is a well-known concern in science, see, e.g., Gundersen and Kjensmo [2018]. Public challenges typically rank the participants by a (single) performance measure, and can fall victims of Goodhart’s law, paraphrased as “When a measure becomes a target, it ceases to be a good measure.” by Teney et al. [2020]. Ma et al. [2021] offered a framework and platform for evaluation of NLP methods, where other aspects such as memory use and robustness are evaluated.

The robustness/stability of a method, and the variability in performance are crucial aspects that the hold-out test set of public challenges does not offer an immediate solution to. Bouthillier et al. [2021] showed empirically that hyperparameter choice and the random nature of the data are two large contributors to variance, whereas data augmentation, dropouts, and weights initialisations are minor contributors. Choice of hyperparameters are often adjusted to validation set results, and the strategies of Blum and Hardt [2015] and Dwork et al. [2017] can hinder that, if implemented by the challenge hosts. Our contribution is a focus on better estimate for SOTA performance under the current conditions, where the approach of Bouthillier et al. [2021] does not apply. Bousquet and Elisseeff [2002] investigated how sampling randomness influences accuracy, both for regression algorithms and classification algorithms, relying on the work of Talagrand [1996] who stated that “A random variable that depends (in a “smooth” way) on the influence of many independent variables (but not too much of any of them) is essentially constant.”

There is a rich literature on various aspects regarding the use of public challenges as standards for scientific publications, see, e.g., Varoquaux and Cheplygina [2022] for a much broader overview than the one given here. Concerns and solutions regarding multiplicity and better performance estimates are active research fields. We contribute to this conversation by shining the light on how multiplicity of classifiers’ performance on hold-out test sets create optimistic estimates of SOTA performance.

3 Multiple classifiers and biased state-of-the-art estimation

3.1 Notation

- n : number of trials/size of test sample
- θ : probability of success
- m : number of experiments/classifiers
- $\mathcal{Bern}(\theta)$: Bernoulli distribution
- Y : indicator variable for success
- $Y \sim \mathcal{Bern}(\theta)$
- $\mathcal{B}(n, \theta)$: binomial distribution
- X : number of failures in one experiment
- $X \sim \mathcal{B}(n, 1-\theta)$
- $\hat{\theta}(X) = \frac{n-X}{n}$: estimator for θ
- $\hat{\theta} = \frac{n-x}{n}$: estimate of θ
- $P(X = x)$: probability of x failures in one experiment
- $P_x = P(X \leq x)$: probability of at most x failures in one experiment
- $\mathbf{X} = \{X_1, X_2, \dots, X_m\}$: number of failures for classifiers $j = 1, \dots, m$
- C_x : number of classifiers with at most x failures
- $C_x \sim \mathcal{B}(m, P_x)$
- Z : the smallest number of failures among all classifiers,
 $z = 0, 1, 2, \dots, n$
- $\Theta = \{\theta_1, \theta_2, \dots, \theta_m\}$: parameters
- $\hat{\Theta} = \{\hat{\theta}_1, \hat{\theta}_2, \dots, \hat{\theta}_m\}$: estimates
- $\theta_{SOTA} = \max(\Theta)$: highest probability of success among all classifiers
- $\hat{\theta}_{SOTA}^{\max}(\mathbf{X}) = \max(\hat{\Theta})$: sample maximum estimator
- α : significance level
- cdf : cumulative distribution function
- pmf : probability mass function

3.2 A coin-flip example

Multiplicity is, simply put, how the probability of an outcome changes when an experiment is performed multiple times.

Consider an experiment where a fair coin is flipped $n = 20$ times and the number of successes is the number of times a classifier correctly predicts the

outcome. Let the random variable X denote the number of failures, $X \sim \mathcal{B}(n, 1-\theta)$, where $\theta = 0.5$. An unbiased estimator for θ is $\hat{\theta}(X) = (n - X)/n$. The corresponding estimate is referred to as accuracy. The probability of, say, 18 correct predictions or more corresponds to $x = n - 18$ failures or less, that is, the cumulative distribution $P(X \leq x | n, 1-\theta)$. This corresponds to the cumulative distribution for the estimator $\hat{\theta}(X) = \frac{n-X}{n}$, and we have that $P(\hat{\theta}(X) \geq \frac{n-x}{n}) = P(X \leq x) = 0.00020$ for $\hat{\theta} \geq 0.90$. In other words, if $\theta = 0.5$, there is a probability of 0.00020 that the accuracy is 0.90 or above in a series of $n = 20$ trials. We can define the experiment described above as a Bernoulli trial, where success is defined as $X \leq x$, with corresponding probability $P(X \leq x)$, which we from now on write as P_x for ease of notation.

If we have m classifiers, we have a series of m Bernoulli trials, and the number of successes follow the binomial distribution $\mathcal{B}(m, P_x)$. Let C_x be the random variable that denotes the number of successful experiments, that is, the number of classifiers that correctly predicts at least $n - x$ coin flips. Of special interest is the case where at least one experiment succeeds, $P(C_x > 0) = 1 - P(C_x = 0)$.

The true SOTA for coin-flip classifiers is $\theta_{SOTA} = 0.5$, since it is impossible to train a classifier to predict coin flips. If $m = 1,000$ classifiers independently give their predictions for $n = 20$ flips, the probability of at least one classifier achieving an accuracy of at least 0.90 is $1 - P(C_x = 0 | m, P_x) = 0.18$. This means that using the top-ranked method as an estimate and ignoring multiplicity there is a substantial risk of grossly overestimating the SOTA.

The same mechanism of multiplicity applies when m teams submit their classifier’s result on a test set, although in a more complex manner. We seek to describe the probability distribution for increasing levels of complexity, and by that offer a tool to avoid overestimation. We will in the following use the public competition as a general example, and refer to the teams’ classifiers simply as classifiers, for ease of notation.

3.3 The probability distribution of $\hat{\theta}_{SOTA}^{\max}(\mathbf{X})$

We define the SOTA probability of success, θ_{SOTA} , as the maximum among the m classifiers being evaluated, $\theta_{SOTA} = \max(\Theta)$, $\Theta = \{\theta_1, \theta_2, \dots, \theta_m\}$. Oftentimes, we only have access to sample estimates, $\hat{\Theta} = \{\hat{\theta}_1, \dots, \hat{\theta}_m\}$. Let $\hat{\theta}_{SOTA}^{\max}(\mathbf{X}) = \max(\{\hat{\theta}_1(X), \hat{\theta}_2(X), \dots, \hat{\theta}_m(X)\})$ be the naive, sample maximum estimator for θ_{SOTA} . In the coin flip classifier example above, we have that $\theta_{SOTA} = 0.5$, but $P(\hat{\theta}_{SOTA}^{\max}(\mathbf{X}) \geq 0.90) = 0.18$, and it is clear that we risk an overoptimistic estimate.

Of interest is $P(\hat{\theta}_{SOTA}^{\max}(\mathbf{X}) | m, n, \Theta)$, which we will denote by $P(\hat{\theta}_{SOTA}^{\max})$ for ease of notation. Similarly, we use $\hat{\theta}_{SOTA}^{\max}$ for $\hat{\theta}_{SOTA}^{\max}(\mathbf{X})$ when there is no risk of confusion. We here give $P(\hat{\theta}_{SOTA}^{\max})$ in the simple case of independent classifiers with identical probabilities of success: $\theta_j = \theta$ for all classifiers, $j = 1, \dots, m$. We discuss non-identical probabilities and dependency in Section 4.

Let X be the random variable that denotes the number of failures (wrong predictions) for a given classifier, with $X \sim \mathcal{B}(n, 1-\theta)$. The random sample,

$\mathbf{X} = \{X_1, X_2, \dots, X_m\}$ consists of the number of wrong predictions for each classifier $j = 1, \dots, m$ on a sample. Let C_x be the random variable that denotes the number of classifiers with at most x failures. We have that $C_x \sim \mathcal{B}(m, P_x)$.

We are interested in the probability of at least one classifier having at most x wrong predictions, because it corresponds to the probability function of the $\hat{\theta}_{\text{SOTA}}^{\max}$ estimator, $P(\hat{\theta}_{\text{SOTA}}^{\max} \geq \frac{n-x}{n})$. We can derive this from $P(C_x > 0 | m, n, \theta)$. This corresponds to the cdf for the random variable Z denoting the most wrong predictions among all classifiers:

$$\begin{aligned} F(z) &= P(C_z > 0 | m, n, \theta) = 1 - P(C_z = 0 | m, P_z) \\ &= 1 - (1 - P_z)^m. \end{aligned} \tag{1}$$

Let $f(z) = P(Z = z)$ denote the pmf of Z , the probability of at least one classifier having exactly z wrong predictions, and no classifiers having fewer than z wrong predictions. We then have

$$\begin{aligned} f(z) &= F(z) - F(z-1) = 1 - (1 - P_z)^m - \{1 - (1 - P_{z-1})^m\} \\ &= (1 - P_{z-1})^m - (1 - P_z)^m = \\ &= \left(1 - \sum_{\ell=0}^{z-1} P(Z = \ell)\right)^m - \left(1 - \sum_{\ell=0}^{z-1} P(Z = \ell) - P(Z = z)\right)^m \\ &= - \sum_{k=1}^m (-1)^k \binom{m}{k} \left(1 - \sum_{\ell=0}^{z-1} P(Z = \ell)\right)^{m-k} P(Z = z)^k. \end{aligned} \tag{2}$$

The variable Z corresponds to $\hat{\theta}_{\text{SOTA}}^{\max}$ in the sense that the smallest number of failures among all classifiers corresponds to the sample maximum probability of success. Equations 1 and 2 can be used to analyse $\hat{\theta}_{\text{SOTA}}^{\max}$ for a given situation, as we do in the next section, where the impact that the three parameters have on the bias is also presented.

3.4 A simulated public competition example

The multiplicity mechanism that we described in the coin-flip example applies to public competitions where multiple teams submit the predictions made by their classifiers on a test set. The classifier with highest performance is declared winner, and is often referred to as SOTA later on. As exemplified in Section 3.2, multiplicity biases the naive sample maximum θ_{SOTA} -estimator, and Section 3.3 gives us the tools to analyze its impact. In the following, we will use a significance level of $\alpha = 0.05$ and two-sided CIs.

Consider a classification problem with a test set of size $n = 3,000$, and a classifier with probability of success $\theta = 0.90$. The pmf of a single $\hat{\theta}(X)$ is shown as the blue curve in Fig. 1, where the dotted line indicates $E(\hat{\theta}) = \theta$. The 95% CI for $\hat{\theta} = 0.90$ is $(0.8887, 0.9105)$, and we denote it by $(\theta_{\alpha/2}, \theta_{1-\alpha/2})$, displayed as a blue line on the horizontal axis.

If there are $m = 1,000$ independent classifiers, each with probability of success $\theta = 0.90$, the probability of at least one classifier achieving at least

$\hat{\theta} = \theta_{1-\alpha/2}$ is close to 1. This comes as no surprise given the definition of a CI. It means that we can be pretty certain that the sample performance of the top ranked classifier is above the upper limit of the CI of the expected performance.

Consider a new classifier with probability of success $\theta_{m+1} = \theta_{1-\alpha/2}$. The corresponding pmf is displayed as the red curve in Fig. 1, with the dotted line indicating $E(\hat{\theta}_{m+1}) = \theta_{1-\alpha/2}$. By common scientific standards, the expected performance is considered significantly better than the expected performance of any of the 1,000 classifiers with $\theta = 0.90$, and is of interest to the research community. However, the multiplicity effect can conceal this. In the competition context, this is not necessarily a problem, since each classifier has the same probability of achieving the highest sample performance given that they have the same θ . In a scientific context, using $\hat{\theta}_{SOTA}^{\max}$ as an estimate for θ_{SOTA} without multiplicity corrections is problematic.

The upper limit of the $(1-\alpha)$ CI of $\hat{\theta}_{SOTA}^{\max}$ is 0.9213, displayed on the horizontal axis in Fig. 1, denoted as $\theta_{1-\alpha/2}^m$. We have $E(\hat{\theta}_{SOTA}^{\max}) = 0.9173$, calculated from Eq. 2, also displayed on the horizontal axis in Fig. 1. The probability of the new classifier beating the upper limit of the sample maximum CI is very low: $P(\hat{\theta}_{m+1} \geq \theta_{1-\alpha/2}^m) = 0.02$, illustrated by the darker green area in Fig. 1. Similarly, $P(\hat{\theta}_{m+1} \geq E(\hat{\theta}_{SOTA}^{\max})) = 0.10$ seen as the entire green area in Fig. 1. This means that by using the sample maximum as an estimator for SOTA, we can expect that 9 out of 10 classifiers that are significantly better will still be naively considered worse. For the entire distribution of $\hat{\theta}_{SOTA}^{\max}$, see Fig. 2.

The distribution of $\hat{\theta}_{SOTA}^{\max}$ will vary with m , n and θ , and Table 1 shows the expectation and standard deviation for a small collection of examples. To complement the table, Fig. 3 a)-c) show the bias of $\hat{\theta}_{SOTA}^{\max}$ as a function of m , n and θ , respectively. For each curve, the two other parameters are kept constant,

Expected values and standard deviations for $\hat{\theta}_{SOTA}^{\max}$

m	n	θ	$E(\hat{\theta}_{SOTA}^{\max})$	$\sigma_{\hat{\theta}_{SOTA}^{\max}}$
1,000	3,000	0.90	0.9173	0.001817
100	3,000	0.90	0.9135	0.002250
5,000	3,000	0.90	0.9196	0.001623
1,000	1,000	0.90	0.9294	0.003007
1,000	10,000	0.90	0.9096	0.001022
1,000	3,000	0.85	0.8707	0.002197
1,000	3,000	0.95	0.9624	0.001277

Table 1: The expected value and standard deviation for the SOTA estimator with varying test set size, number of classifiers and probability of correct success. The bold line is the example used in Fig. 2 and corresponds to the intersection between the gray vertical lines and the solid lines in Fig. 3.

and each figure displays five curves, corresponding to Table 1.

In Fig. 3a, we see that the impact of number of classifiers is dramatic, and

The pmfs of two single $\hat{\theta}(X)$ compared to $\hat{\theta}_{\text{SOTA}}^{\max}$ statistics

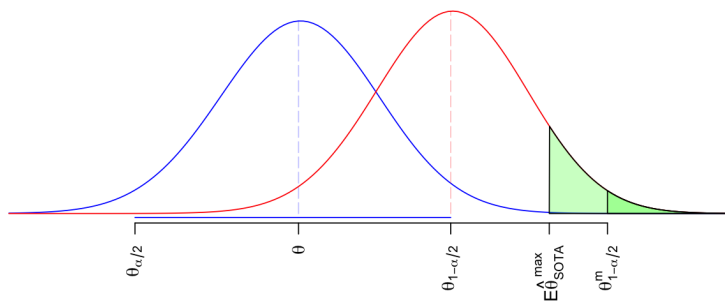


Figure 1: Against a mass of identical classifiers, a single significantly better classifier has little chance of beating the state of the art: The blue and the red curves show the pmfs of $\hat{\theta}(X)$ for classifiers with probability of success θ and $\theta_{1-\alpha/2}$, respectively. $\theta_{1-\alpha/2}$ is the upper limit of the CI of $\hat{\theta}(\mathbf{x}) = \theta$. The CI is displayed as the blue horizontal line. $E(\hat{\theta}_{\text{SOTA}}^{\max})$ and $\theta_{1-\alpha/2}^m$ denote the expected value and the upper limit of the CI of the sample maximum estimator for $m = 1,000$ classifiers. The shaded areas corresponds to $P(\hat{\theta}_{m+1} \geq \theta_{1-\alpha/2}^m)$ and $P(\hat{\theta}_{m+1} \geq E(\hat{\theta}_{\text{SOTA}}^{\max}))$, and reflects the slim chances that the single better classifier has of beating the multiple worse classifiers.

multiplicity-considerations must be treated with full attention starting at $m = 2$. We can see this from the cdf in Eq. 1, where m is the exponent. In Fig. 3b that the test set size also has large impact on the bias. With small test sets, the variance of each individual $\hat{\theta}_j(X)$ is high, increasing the probability of sample estimates far from θ . As seen in Fig. 3c, the bias decreases as θ approaches 1. The variance of the individual $\hat{\theta}_j(X)$ s is at its highest for $\theta = 0.5$ and decreases monotonically, and it is this variance that is reflected in the bias, similar to the effect of the test set size.

The change in absolute numbers may seem modest, but the practical implications are large, as demonstrated in Section 5, where we analyse the results from three public competitions.

4 Dependency and non-identical θ s

The probability distribution in Section 3.4 is that of independent classifiers with identical θ s, an assumption that is rarely true in practice. We expand our investigation to non-identical θ s and dependency. Table 2 and Figure 5 give

**Cdf and pmf for at least one classifier having at most z failures,
corresponding to the sample maximum estimator**

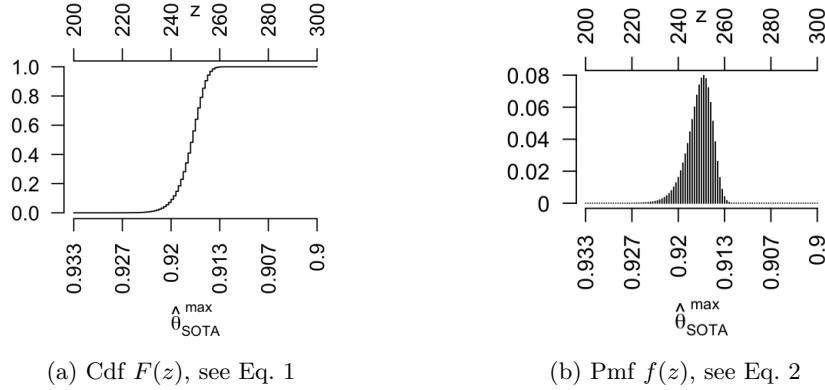


Figure 2: The distribution and the probability function of the sample maximum estimator for $n = 3,000$, $\theta = 0.90$, and $m = 1,000$. The horizontal axes denotes the number of failures, z , at the top and the corresponding sample maximum estimates, $\hat{\theta}_{\text{SOTA}}^{\max}$, at the bottom. Note that the horizontal axis is reversed compared to Fig. 1.

The bias of the sample maximum estimator

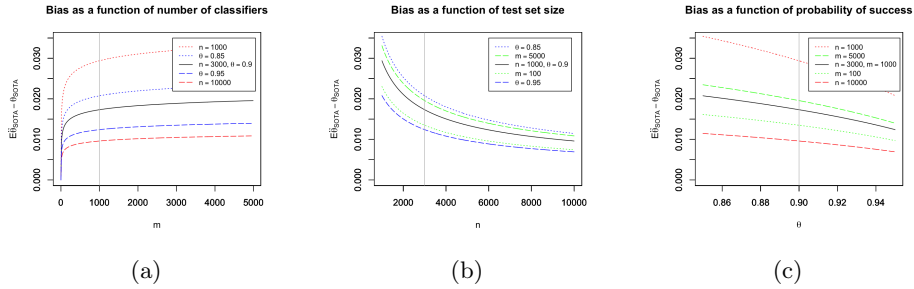


Figure 3: The bias of $\hat{\theta}_{\text{SOTA}}^{\max}$ as a function of each of its three parameters; number of classifiers, test set size and probability of success. The intersection between the black solid lines and the gray vertical lines correspond to the bold line in Table 2. The dotted and dashed lines correspond to variation of parameter values found in Table 2, colour-coded accordingly.

an overview of some exemplifying models, details are in the following sections.

Overall, Table 2 demonstrates that dependency and non-identical θ s reduces the bias of the $\hat{\theta}_{\text{SOTA}}^{\max}$ estimator, and assumptions regarding dependency and identity are crucial to include in a model. Figure 4 shows how the bias

Characteristics of $\hat{\theta}_{\text{SOTA}}^{\max}$ for dependent and non-identical classifiers

Section	Independent	Identical	Upper 95% CI	$E(\hat{\theta}_{\text{SOTA}}^{\max})$	$\sigma_{\hat{\theta}_{\text{SOTA}}^{\max}}$
3.4	YES	YES	0.9213	0.9173	0.0018
4.1	YES	NO	0.9177	0.9130	0.0021
4.2	NO	YES	0.9207	0.9140	0.0035
4.3	NO	NO	0.9173	0.9101	0.0036

Table 2: The upper bound of the 95% CI, the expected value and standard deviation for the sample maximum estimator for different combinations of independency and identity. The true SOTA is $\theta = 0.90$, the test set size is $n = 3,000$, the number of classifiers is $m = 1,000$. The correlation coefficient and the Θ -vector are found in their respective subsections.

changes as a function of Θ and ρ_0 for these specific models.

We use the set-up from Section 3.4 with $m = 1,000$ classifiers, test set size $n = 3,000$, $\theta_{\text{SOTA}} = 0.90$, and 100,000 repetitions when simulations are needed. We refer to classifiers with identical θ s as identical classifiers.

4.1 Non-identical, independent classifiers

We are interested in generalising Eq. 1 to the non-identical case, and we start by noting that we now have $P_{xj} = P(X \leq x|\theta_j)$, and we seek the sum of those so that we can find the proper expression for

$$F(z|\Theta) = 1 - P(C_z = 0|m, n, \Theta).$$

The Poisson Binomial distribution, see, e.g., ?, describes the sum of m non-identical independent Bernoulli trials with success probabilities p_1, p_2, \dots, p_m . The pmf for K number of successes is

$$P(K = k) = \sum_{A \in G_k} \prod_{i \in A} p_i \prod_{j \in A^c} (1 - p_j), \quad (3)$$

where G_k is all subsets of size k that can be selected from $\{1, 2, \dots, m\}$.

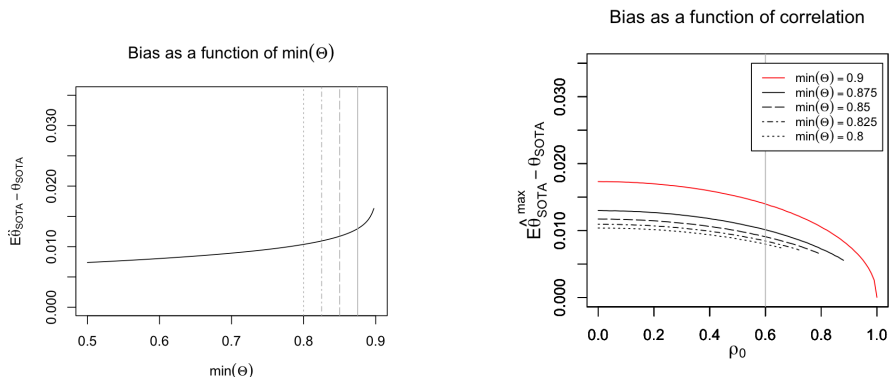
We then get the cdf for non-identical classifiers

$$F(z|\Theta) = 1 - \sum_{A \in G_0} \prod_{i \in A} P_{zi} \prod_{j \in A^c} (1 - P_{zj}) = 1 - \prod_{j=1}^m (1 - P_{zj}). \quad (4)$$

The pmf is

$$\begin{aligned} f(z|\Theta) &= \prod_{j=1}^m (1 - P_{z-1j}) - \prod_{j=1}^m (1 - P_{zj}) \\ &= \prod_{j=1}^m \left(1 - \sum_{k=0}^{z-1} \binom{n}{k} (1 - \theta_j)^k \theta_j^{n-k}\right) - \prod_{j=1}^m \left(1 - \sum_{k=0}^z \binom{n}{k} (1 - \theta_j)^k \theta_j^{n-k}\right). \end{aligned} \quad (5)$$

Bias for non-identical and dependent classifiers.



(a) Bias as a function of $\min(\Theta)$, with constant $\max(\Theta) = 0.90$

(b) Bias as a function of correlation coefficient.

Figure 4: Bias of the sample maximum estimator as a function of $\min(\Theta)$ for non-identical classifiers and of ρ_0 for conditional independent classifiers. (a) The right tip of the curve is identical classifiers, and following the curve from right to left the Θ -vector stretches out, and the bias decreases. The intersection with the solid gray vertical line corresponds to the cdf and pmf in Fig. 5, and produces the CI, the expectation and the standard deviation in line two in Table 2. The intersections between the gray vertical lines correspond to the left tips of the black lines in Fig. 4b, where the classifiers are independent. (b) The red line are identical classifiers, as discussed in Section 4.2. The left tip of the red curve corresponds to the i.i.d. classifiers in Section 3.4, and the intersection with the grey vertical line corresponds to line three in Table 2. The black lines show bias as a function of correlation coefficient demonstrated for different Θ -vectors. The intersection between the solid black curve and the grey vertical line corresponds to line four in Table 2. The scale of the y -axis is kept the same as in Fig. 3 for easier comparison of which parameters have the most impact.

Analytically, it is more complex than the case of identical classifiers, but it is easy to simulate.

We use the same parameters as in Section 3.4, replacing $\theta = 0.90$ with the vector Θ , where $\min(\Theta) = 0.875$, $\max(\Theta) = 0.90$ and equally spaced elements. The cdf and pmf are displayed in Fig. 5a and Fig. 5b.

The upper bound of the 95% CI is 0.9177. The $E(\hat{\theta}_{\text{SOTA}}^{\max})$ is 0.9129, with standard deviation of 0.0021. Comparing this to the results in Section 3.4, we see that the bias is smaller and the variance larger. This is because the classifiers at the lower end does not contribute to the sample maximum, and the reduced number of contributing classifiers gives a higher variance. The exact reduction/increase in bias and variance depends on Θ , and can at its most

Cdf and pmf for non-identical classifiers.

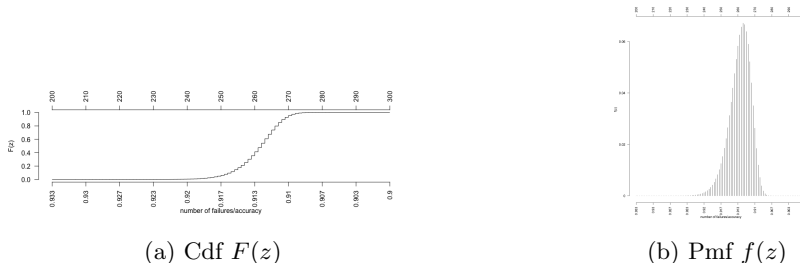


Figure 5: The distribution and the probability function of the sample maximum estimator for non-identical θ s, where $\min(\Theta) = 0.875$, $\max(\Theta) = 0.90$ and equally spaced elements.

extreme cases completely eradicate the multiplicity effect, as we shall see in Section 5.1.2. Figure 4a shows how $E(\hat{\theta}_{\text{SOTA}}^{\max})$ changes with $\min(\Theta)$ for equally spaced elements with $\max(\Theta) = 0.90$.

What we see here is that with non-identical classifiers the bias decreases rapidly at first as $\min(\Theta)$ moves away from $\max(\Theta)$, but the rate at which this happens also decreases rapidly. This means that taking into account that classifier performances are heterogeneous is important, and small variations from identity can have great impact on SOTA estimation. In Section 5, we demonstrate for other Θ s, based on observations.

4.2 Identical, dependent classifiers

Even though the different teams work independently, their resulting classifiers are not necessarily statistically independent. A classifier’s ability to perform better than random guesses is due to the correlations between features and labels in the training set. In their training phase, different classifiers will pick up on many of the same features and correlations, regardless of which classifier they train. In addition, many teams will use different versions of related models, often pre-trained on the same data set. This scenario can be modelled by conditional independency.

Let Y_0 be a Bernoulli variable with $P(Y_0 = 1) = \theta_0$. Let Y_j be the Bernoulli variable with value 1 if classifier j predicts a data point correctly with $P(Y_j = 1) = \theta_j$, and let $j = 1, \dots, m$ be the m classifiers contributing to $\hat{\theta}_{\text{SOTA}}^{\max}$. Boland et al. [1989] described dependency in the majority systems context, where $\rho_{0j} = \text{corr}(Y_0, Y_j)$, $j = 1, \dots, m$, and the Y_j s are independent given Y_0 . The observations from Y_0 does not contribute directly to $\hat{\theta}_{\text{SOTA}}^{\max}$, but can be seen as, e.g., the influence that a common training set has on the classifiers.

The binomial distribution for dependent Bernoulli trials is not an easy problem, see, e.g., Ladd [1975] and Hisakado et al. [2006]. The Bernoulli trials can be simulated, see Boland et al. [1989] for conditional distributions. We give an

example below for the case where $\rho_{0j} = \rho_0$ and $\theta_j = \theta$ for all classifiers. We set ρ_0 based on the work of Mania et al. [2019].

Mania et al. [2019] calculated model similarity, defined as the probability of two classifiers giving the same output, which is equivalent to

$$(1 - \theta_j)(1 - \theta_k) + \theta_j\theta_k + 2\rho_{jk}\sqrt{\theta_j\theta_k(1 - \theta_j)(1 - \theta_k)} \quad (6)$$

for dependent models with correlation ρ_{jk} . The average accuracy for top-performing ImageNet models, $\hat{\theta} = 0.756$, and the calculated similarity of 0.85 gives $\rho = 0.36$ if we assume the same correlation for all classifiers. We have that $\rho_{jk} = \rho_{0j}^2$, and hence our proposed correlation ρ_0 is set to 0.6. Note that, for $\theta = 0.90$, the similarity as described by Mania et al. [2019] is 0.82 for two independent classifiers. When the probability of correct prediction is high, there is little room for variation between classifier outcomes.

Let $P(Y_j = 1) = \theta = 0.90$ for all classifiers, and $P(Y_0 = 1) = \theta = 0.90$. From our simulations, we get $E(\hat{\theta}_{\text{SOTA}}^{\max}) = 0.9140$, a decrease in bias compared to the independent and identical classifiers. However, the variance has increased due to the random nature of Y_0 , so the upper 95% CI is essentially the same. See, Table 2 for exact numbers.

To give an idea of how the randomness of Y_0 influences the variance, we fix the y_0 's with exactly $(n - x)/n = 0.90$ correct predictions. The expected value is the same as with random Y_0 's, but the standard deviation has now decreased from 0.0035 to 0.0015. In the real world, the dependencies have both random and fixed sources. A random source would, e.g., be the training set and the test set, random samples from an underlying distribution. A fixed source can be, e.g., fixed training conditions, such as pre-trained models.

For $\rho_{0j} = 0$, we have independent classifiers, the same scenario as in Section 3.4, and for $\rho_{0j} = 1$, we have m classifiers producing the same output, and multiplicity is not a concern. For the whole range, see the red curve in Figure 4b.

What we see here is that the correlation coefficient value in a model has a great impact on the estimated bias if the correlation is substantial. This can explain that in mature fields, where most competing teams will use variants of the same model, the multiplicity will not impact the overestimation of SOTA as much as in young fields where the competing teams have more diverse models. This aligns with what is often observed in science: overoptimistic results in the beginning, and more sober as the field evolves.

4.3 Non-identical, dependent classifiers

The most complex, but also the most realistic case, is where classifiers are non-identical and dependent. An analytical solution is not known Hisakado et al. [2006], but simulations are straightforward. The results of Boland et al. [1989]

can be extended, and we have that

$$P(Y_j|Y_0 = 1) = \frac{\rho\sqrt{\theta_j(1-\theta_j)\theta_0(1-\theta_0)} + \theta_j\theta_0}{\theta_0} \quad (7)$$

$$P(Y_j|Y_0 = 0) = \frac{-\rho\sqrt{\theta_j(1-\theta_j)\theta_0(1-\theta_0)} + \theta_j(1-\theta_0)}{(1-\theta_0)}. \quad (8)$$

Note that, since $P \leq 1$, it follows from Eq. 8 that

$$\theta_j \geq \frac{\rho^2 \frac{\theta_0}{1-\theta_0}}{1 + \rho^2 \frac{\theta_0}{1-\theta_0}}, \quad (9)$$

and similarly for $0 \leq P$ and Eq. 7.

We get an upper bound of the 95% CI of 0.91733 and an expected value of 0.9101, which are lower than both the dependent and the non-identical model separately. The standard deviation is 0.0036, which is higher than the two other models. This sums of up much of Table 2, where more complex, and therefore more realistic, models reduces the bias but increases the variances.

Figure 4b shows the impact of correlation for non-identical classifiers. What we see is that the bias decreases slowly for low correlations, but that the rate increases as ρ_0 increases. Importantly, Eq. 9 restricts the discrepancy between $\min(\Theta)$ and $\max(\Theta)$, and the graphs are right-truncated. From Fig. 3a we observe that the impact from number of classifiers flattens off, instead of restricting ρ_0 in our model, we can exclude classifiers by performance without large effect on the estimated bias. That is, restricting $\min(\Theta)$ instead of ρ_0 . What we also observe in Fig. 4a is that change in $\min(\Theta)$ has less impact on the lower end of the scale, so this also supports a decision of excluding teams with low performance without impacting the bias-estimation too much.

5 Real world examples

As we have shown above with simulated data, the sample maximum is an overoptimistic estimate for SOTA. These results are based on known SOTA, but faced with real world data the problem to be solved is of opposite nature: The sample $\max(\hat{\Theta})$ is known, but the true SOTA must be estimated. In the public competition or public data set context there are many factors that come in to play, making the bias calculations everything but straightforward.

We here demonstrate different aspects of real world analysis through SOTA estimation of three different cases: Obesity Risk (5.1.1), Cassava Leaf (5.1.2, and Melanoma (5.2). Obesity Risk and Cassava Leaf have accuracy, defined as $\hat{\theta}$, as their ranking criterion, whereas Melanoma has area under the receiver operating characteristic (ROC) curve (AUC) as ranking criterion. To estimate multiplicity effect on the AUC scores is not as straightforward as with accuracy, but the mechanisms are the same and AUC is a more common ranking criterion than accuracy.

In a public competition with m participating teams, let $\hat{\Theta} = \{\hat{\theta}_1, \hat{\theta}_2, \dots, \hat{\theta}_m\}$, be the estimated probability of success for each classifier based on the performance on an independent test sample of size n . The the winning team is identified by the sample maximum, $\max(\hat{\Theta})$. Among the different scenarios presented in Section 4, the non-identical dependent is the most realistic model. Whereas in Table 2 we report $E(\hat{\theta}_{SOTA}^{max})$ from known Θ , the task is now to estimate θ_{SOTA} based on $\hat{\Theta}$. A straightforward approach is to find $\Theta' = \{\theta'_1, \theta'_2, \dots, \theta'_m\}$ that gives $E(\max(\hat{\Theta}')) = \max(\hat{\Theta})$. That is, find a set of θ 's so that the expected value of its sample maximum on a test set of size n is equal to the competition sample maximum. The SOTA estimate is then $\max(\Theta')$. We use a set-up where the simulated $\hat{\theta}'_j$ s are the mean values of n realisations of Y_j , where $P(Y_j) = \theta'_j$. The simulation is repeated 10,000 times, and for each repetition the observed maximum value is recorded. $E(\max(\hat{\Theta}'))$ is the mean value over the repetitions.

In the studies in Section 4, the $\theta_1, \dots, \theta_m$ were chosen to be equally spaced, but this does not align with the real world sample estimates, as seen in Figures 6a, 7a and 8. We base our suggested θ'_j 's on cropping the sample estimates, as seen, e.g., in Figure 6c, but this is far from the only approach. Shrinking, which we also investigated, might give a more realistic set of θ'_j 's, but it also requires an extra parameter. For the examples presented here shrinking gave similar results to cropping, and are therefore not included.

An alternative to the expected value of the sample maximum is the upper limit of the 95% CI. The latter is more in line with common interpretation of the uncertainty of observed results in research, but which to choose will depend on the aim of the analysis. We demonstrate the impact in the Obesity Risk example, reported in Table 3.

Not every $\max(\hat{\Theta})$ is a result of multiplicity, and we demonstrate this in the Cassava Leaf example.

5.1 Estimating θ_{SOTA}

5.1.1 Multi-Class Prediction of Obesity Risk

Multi-Class Prediction of Obesity Risk is a competition in the 2024 Kaggle Playground Series, using a synthetic data set generated from the *Obesity or CVD risk* data set [Palechor and de la Hoz Manotas, 2023]. The test sample size was $n = 13,840$, and the number of participating teams were $m = 3,498$ (excluding teams with accuracy lower than chance). The maximum sample estimate was $\max(\hat{\Theta}) = 0.9116$. Figure 6a shows the sample estimates, $\hat{\theta}_j$'s, zoomed in at the 3,081 classifiers with sample estimates above 0.88. The 95% CI for $\hat{\theta} = 0.9116$ is (0.9067, 0.9162) and is shown as the red line in Figure 6a, the lower bound enveloping 920 of the sample estimates. This should raise suspicion that the right tail seen in Figure 6a can be the product of multiplicity.

To demonstrate the impact of ignoring multiplicity, let $\theta'_1, \dots, \theta'_m$ be equal to the sample estimates and calculate the expected value of the sample maximum, $E(\max(\hat{\Theta}'))$. We use the set-up from Section 4.3 with correlation coefficient $\rho_0 = 0.6$, and $P(Y_0) = \theta_0 = \max(\Theta')$. Note that sample estimates with low

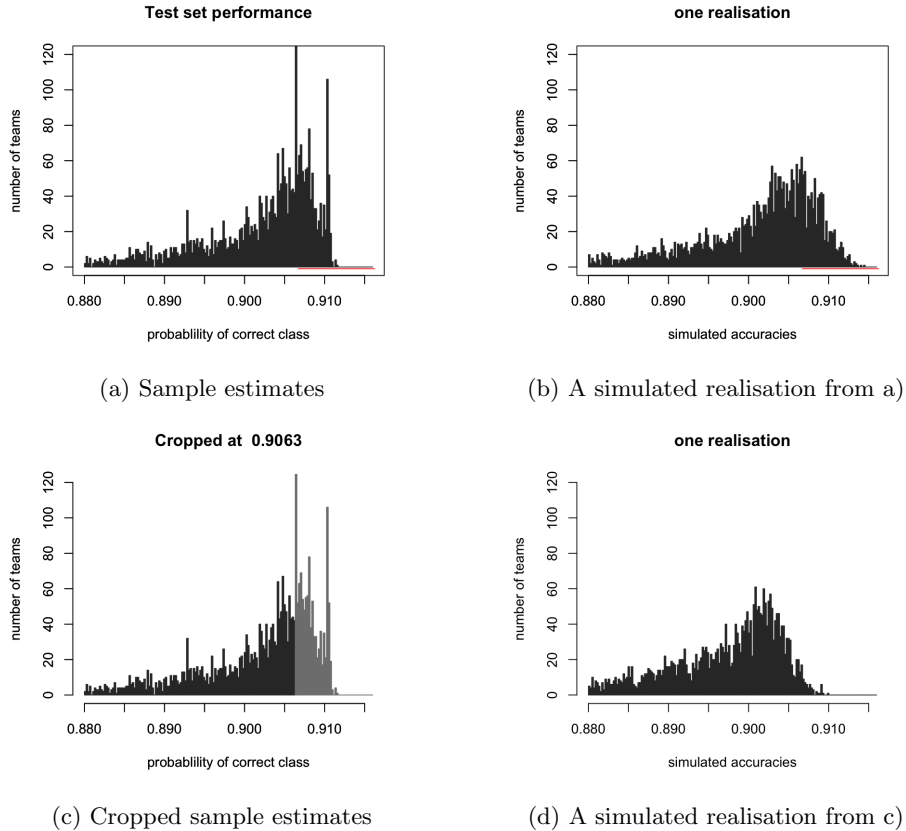


Figure 6: The competition observations and simulated realisation of classifiers with corresponding probabilities of correct classification. The red line is the 95% CI for $\hat{\theta}^{\max}$ in (a).

values are excluded in accordance with Eq. 9, but their influence on the expected maximum is negligible.

A realisation is shown in Figure 6b. The upper tail, whose tip represents the maximum sample estimate, is stretched according to the variances of the Y_j s. The estimated expected sample maximum is $E(\max(\hat{\Theta}')) = 0.9159$, far above the sample maximum in the competition. The 95% CI is reported in Table 3. The lower bound exceeds $\max(\hat{\Theta})$, and we can conclude that the sample maximum is an unlikely candidate for SOTA. The CI is calculated by $B = 1,000$ bootstrap samples of size m drawn from the sample estimates, and then the simulation as described above is conducted for each bootstrap sample.

Instead, we can find a set Θ' that results in realisations, $\hat{\Theta}'$, similar to the competition sample estimates in terms of sample maximum, and let $\max(\Theta')$ be the SOTA candidate. To obtain a set Θ' where $E(\max(\hat{\Theta}')) = \max(\hat{\Theta})$,

we crop the competition sample estimates, as seen in Figure 6c, and where $E(\max(\hat{\Theta}'))$ is calculated from simulations as described above. Figure 6d shows one realisation of the cropped distribution, where $\max(\hat{\Theta}')$ is close to $\max(\hat{\Theta})$. By cropping at 0.9062 we obtain $E(\max(\hat{\Theta}')) = \max(\hat{\Theta})$, and this serves as a new candidate for the SOTA.

It can be argued that the new SOTA candidate is at risk of being an optimistic estimate, since the competition observations are from only one test sample. The upper bound of the 95% CI can mitigate such a risk, and the competition sample estimates are cropped to fit that criterion. The CI is calculated by bootstrapping, as described above. The results are shown in Table 3.

Estimating θ_{SOTA}

Approach	$\max(\Theta')$	95% CI	$E(\max(\hat{\Theta}'))$	# teams
no mult.	$\max(\hat{\Theta})$	(0.9067, 0.9162)	-	-
$\Theta' = \hat{\Theta}$	$\max(\hat{\Theta})$	(0.9128, 0.9191)	0.9159	-
cropping	0.9062	(0.9084, 0.9148)	$\max(\hat{\Theta})$	1134
	0.9026	(0.9050, $\max(\hat{\Theta})$)	0.9083	1844

Table 3: The 95% CI and the expected value for sample maximum, $\max(\hat{\Theta}')$, for different SOTA estimation strategies, where SOTA is defined as $\max(\Theta')$. The competition sample maximum is $\max(\hat{\Theta}) = 0.9116$. The bootstrap standard deviations are in the order of magnitude 10^{-5} - 10^{-4} , and are therefore not displayed. The rightmost column shows number of classifiers with sample performance above the estimated SOTA.

Table 3 demonstrates that taking the effect of multiplicity into account changes how results are perceived dramatically. The new SOTA value is 0.9062, and even though its reduction from best performance is only about 0.005, the effect it has on who we consider performing at SOTA-level is dramatic: around one third of the classifiers have sample performance above the new SOTA. The more conservative approach using the upper bound of the 95% CI to estimate SOTA gives an even more dramatic result, and either way the impact is substantial.

5.1.2 Cassava Leaf Disease

In this example, the maximum sample estimate is unlikely to be the product of multiplicity. For The Cassava Leaf Disease Classification competition, the task was to classify images of cassava leaves. The training set consisted of 21,367 labelled images of five classes, and the test set of approximately 15,000 images. 3,752 teams participated (excluding those with sample performance lower than chance).

The three top performances appear as outliers (0.9132, 0.9043 and 0.9028) as seen in Figure 7a. Several explanations for the outlying performances of the three top teams have been put forward, and the interested reader can take a

deep-dive in the comment section of the competition. Since this is not the topic of the present work, we will not engage in the discussion here. The 95% CI of $\hat{\theta} = 0.9132$ is $(0.9086, 0.9177)$, no other sample performance is within this interval. By performing simulations without cropping, we get $E(\max(\hat{\theta}')) = \max(\hat{\Theta})$, and although the upper tail is stretched, its tip does not surpass $\max(\hat{\Theta})$.

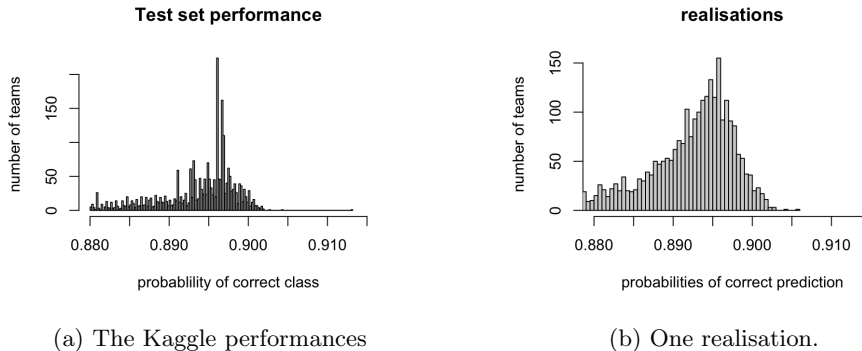


Figure 7: Cassava Leaf sample performances and one realisation.

This analysis demonstrates that the suggested approach for SOTA estimation is robust in the sense that when multiplicity is not a likely explanation to the sample maximum value, the SOTA value is not altered by this approach.

5.2 Estimating AUC_{SOTA}

5.2.1 Melanoma Classification

We will use the Melanoma Classification competition from 2020 as an illustrative example of AUC_{SOTA} estimation because it follows many of the common structures of public challenges. The results are presented in Section 5.2.3.

The SIIM-ISIC Melanoma Classification competition consisted of more than 40,000 images of skin lesions from various sites, split into training (33,126), validation (3,295) and test set (7,687). The data set is highly imbalanced, with less than 2% melanomas, which reflects the reality in many cancer detection situations. A full description can be found in Rotemberg et al. [2021]. The size of the test set is smaller than the recommendations of, e.g., Roelofs et al. [2019], but reflects the reality of benchmark datasets and public challenges, as seen in, e.g., the overview of Willemink et al. [2020]. We want to emphasise that the shortcomings of this competition are not unique, and that is precisely why it serves as a useful example.

Participants were allowed to use additional data for training if the data was shared on the competition web site. The prize money was set to 10,000 USD for the best-performing method, measured as AUC on the hold-out test set. Figure 8 shows the results. Participants could get intermediate results from the validation set, published on a public leaderboard.

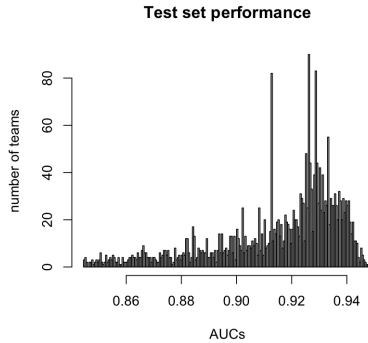


Figure 8: AUCs for the Melanoma Classification competition, calculated on a hold-out test set, cropped from below for better visualisation.

The team ‘All Data Are Ext’, consisting of three Kaggle Grandmasters, won the competition, achieving an AUC of 0.9490 on the test set, and their method and strategy is explained in Ha et al. [2020]. Although we show that the AUC is an optimistic estimate for the melanoma detection SOTA, we do not question their rank in the challenge. Quite the contrary; the winning team chose many of the verified strategies from Section 2. They used additional data from previous years’ competitions, and they also did data augmentation. They chose ensemble learning as a strategy to avoid overfitting, a strategy implicitly supported by Talagrand [1996]. They also trained on multiple classes, a strategy that Feldman et al. [2019] showed will slow down the overfitting.

In the following sections, we introduce a strategy for estimating AUC_{SOTA} , using simulated examples and the Melanoma Challenge for illustration.

5.2.2 Simulation of AUC

In a binary classification problem, the calculation of AUC is based on scores of random variables from the positive and the negative class. The AUC is mathematically equivalent to the probability that a random variable from the positive class will be ranked higher, in terms of score, than a random variable from the positive class [Hanley and McNeil, 1982].

Let $score(\cdot)$ be a function that assigns a score to a random variable. Let $S_+ = score(W_+)$, where W_+ is a random variable from the positive class, and $S_- = score(W_-)$, where W_- is a random variable from the negative class. Then $AUC = P(S_- < S_+) = P(S_- - S_+ < 0)$, which is equivalent to the cdf at value 0. To simulate classifier scores according to a given $AUC = a$, we need to specify distributions for the variables S_- , S_+ in such a way that $P(S_- - S_+ < 0) = a$. We use Normal distributions for illustration.

Let S_+ and S_- have the distributions

$$S_+ \sim \mathcal{N}(\mu_+, \sigma_+^2) \tag{10}$$

$$S_- \sim \mathcal{N}(\mu_-, \sigma_-^2), \tag{11}$$

where $\mathcal{N}(\mu, \sigma^2)$ is the Normal distribution with mean μ and variance σ^2 . We then have that

$$\text{AUC} = \Phi \left(\frac{0 - (\mu_- - \mu_+)}{\sqrt{\sigma_-^2 + \sigma_+^2}} \right), \tag{12}$$

where Φ is the cdf of the standard Normal distribution. Specifying any three of the four parameters above decides the last one for a chosen $\text{AUC} = a$. Figure 9a shows an example where $\text{AUC} = 0.90$.

The distribution of classifier scores, S , is a mixture distribution of the S_+ and the S_- distributions, where the weights, π and $1 - \pi$, correspond to the probability of selecting a positive or a negative random sample, and has pdf

$$\pi f_+(s) + (1 - \pi) f_-(s), \tag{13}$$

where $f_+(s)$ and $f_-(s)$ are the pdfs of the positive and the negative class, respectively. Expected value and variance of S are

$$\mu = \pi \mu_+ + (1 - \pi) \mu_-, \text{ and} \tag{14}$$

$$\sigma^2 = \pi(\sigma_+^2 + \mu_+^2) + (1 - \pi)(\sigma_-^2 + \mu_-^2) - \mu^2. \tag{15}$$

Figure 9a shows an example of Normally distributed negative and positive scores and an AUC of 0.90. The rug shows an example draw with $n = 3000$ and $\pi = 0.017$, corresponding to the class balance in the Melanoma challenge.

The choice of distributions has an impact on the final SOTA estimation, as it affects the variance of the ROC curves. However, with high AUC, the shape has less impact, and the analyst's choices are not suggestive of the overall conclusion.

5.2.3 Simulation results for uncorrelated classifiers

To demonstrate the impact that multiplicity can have in a public competition, we start with a simulated example similar to the one in Section 3.4. Consider a classification problem with a test set of size $n = 3,000$, number of participating teams, $m = 1,000$, where each classifier has a true underlying AUC of $a = 0.90$, and the classifiers are independent.

Whereas the distribution of the sample maximum for probability of success is independent of class balance as long as the probability of success is independent of class, this is not true for the sample maximum of AUC, where the variance increases with class imbalance. We have chosen the same class balance as in the

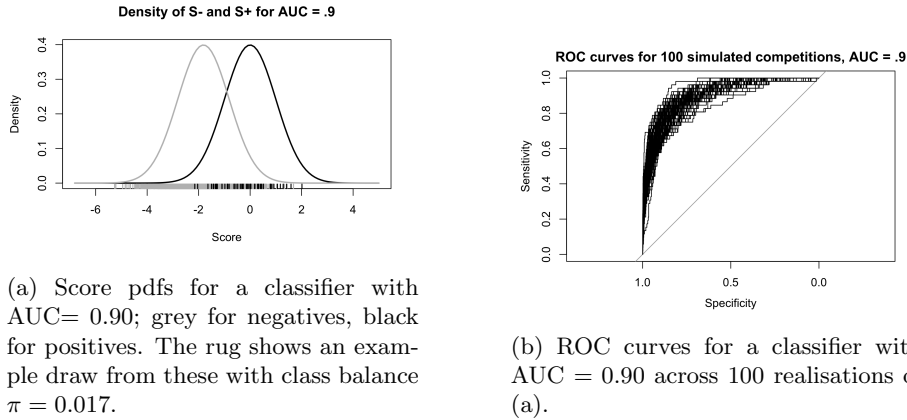


Figure 9: Example of what an AUC of 0.90 might look like in practice. The right figure shows 100 realizations of a ROC curves. The left figure shows the underlying score distributions that generated the curves in (b).

Melanoma challenge, $\pi = 0.017$, as this reflects real world examples. For simplicity we choose $\mu_- = 0$ and $\sigma_- = \sigma_+ = 1$. We then solve for μ_+ numerically. Now we can generate scores from the resulting Normal distribution. The 95% CI of a single classifier with $\hat{AUC} = 0.90$ is $(.8558, 0.9376)$, and gives a strong indication of what we can expect when 1,000 teams apply their classifiers on a test set.

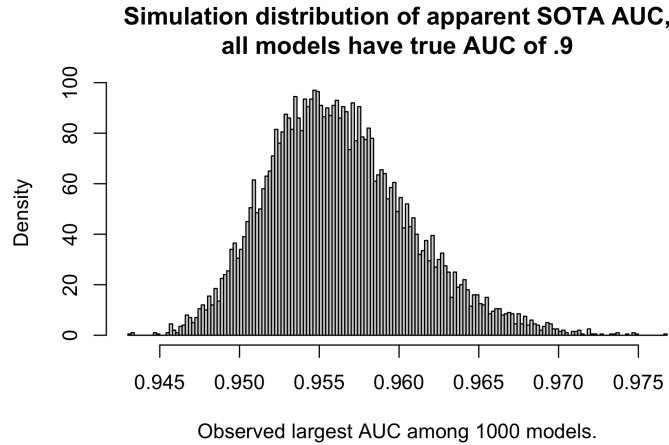


Figure 10: Simulated distribution of the sample maximum AUC with parameters as in Figure 9. This is an analogous figure to Figure 2b in Section 3.4.

Figure 10 shows the simulated distribution of the sample maximum AUC over 10,000 repetitions of a competition where every classifier has a true AUC of 0.90. The simulated expected value is 0.9562, the standard deviation is 0.004459, and the simulated 95% CI is (0.9486, 0.9662). Comparing this to the results in Section 3.4, we see that the bias is much larger for the sample maximum AUC. This is partly due to the large variance created by the class imbalance. Although the sample size is $n = 3,000$, only 51 of those belong to the positive class, creating large variance in the estimator.

Again, it is clear that the observed maximum is an unlikely SOTA candidate, and to give a better estimate of the SOTA for the Melanoma challenge, we follow the same procedure as in Section 5.1: The competition sample estimates are cropped in such a manner that their realisations give an expected value of 0.9490, the competition sample maximum.

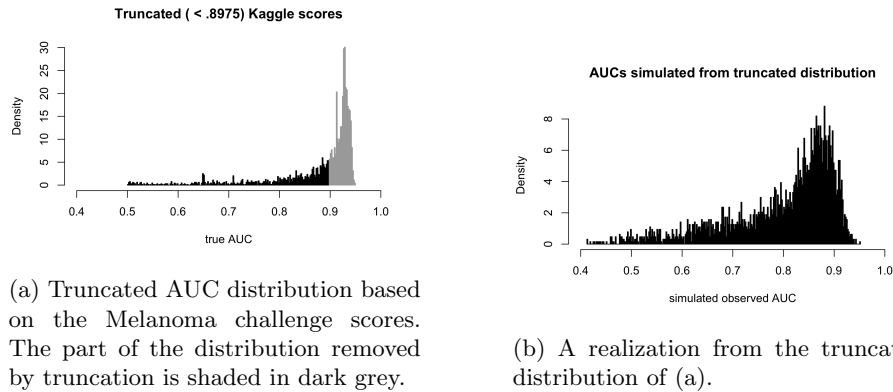


Figure 11: Histogram of cropped competition AUC sample estimates. Here the state of the art is an AUC of 0.8975 which leads to the expected sample maximum AUC of 0.9490.

Figure 11a shows one bootstrap sample from the kaggle observations cropped at 0.8975. Number of classifiers is set to $m = 3,173$, which is as many as there are classifiers in the melanoma challenge with $\text{AUC} > 0.5$. Figure 11b shows a corresponding realisation, where the maximum is close to 0.9490. There are 2,022 teams with performance above the new SOTA candidate.

The discrepancy between the sample maximum and the new SOTA candidate is big, and have big implications. From an AUC close to 95% to just under 90% is a substantial drop in performance in a cancer detection setting. In addition, two-thirds of the classifiers have performances above the new SOTA estimate. As was shown in Section 4, illustrated in Figure 4b, the bias is reduced for correlated classifiers, so the analysis with independence assumption is an overestimation of the bias. In this challenge, we can assume multiple sources of dependency: Access to the same training set, models pre-trained on the same data, similar models, etc. However, the wide CI for a single classifier tells the story of an

estimator with large variance, and hence, the bias of the sample maximum will be substantial.

5.2.4 Correlation between classifiers in the AUC simulations

For the moment we have not extended our AUC simulations to include correlations, but it should be possible to adopt a similar setup as in Sections 4.2 and 4.3: each classifier produces scores that correlate to those of a reference classifier. Let S_{0+} and S_{0-} be the scores of the reference classifier, for random variables from the positive and negative class, respectively.

Let $\rho_+ = \text{corr}(S_{0+}, S_{j+})$ be the correlation between the reference classifier scores S_{0+} and the scores of classifier j , S_{j+} for the positive class. If they both follow Normal distributions as outlined above, then the bivariate distribution is

$$\begin{pmatrix} S_{0+} \\ S_{j+} \end{pmatrix} \sim \mathcal{N} \left(\begin{pmatrix} \mu_{0+} \\ \mu_{j+} \end{pmatrix}, \begin{pmatrix} \sigma_{0+}^2 & \rho\sigma_{0+}\sigma_{j+} \\ \rho\sigma_{0+}\sigma_{j+} & \sigma_{j+}^2 \end{pmatrix} \right),$$

and equivalently for the negative class. However, the joint distribution of (S_0, S_j) is not uniquely defined by the correlation, and additional assumptions must therefore be made. We leave this as future work.

6 Discussion

We have addressed the mechanisms of multiplicity and how they affect the bias of the SOTA estimator. When probability of success is used as a performance measure, the exact distribution of the sample maximum estimator can be provided in the simpler cases, and known analyses methods can be engaged. The bias in SOTA is substantial in our examples, and possibly hinders new methods to attract interest from the scientific community.

We have presented the simple case with an analytical solution, where the probabilities of correct prediction are known.

We have also presented three case-studies from Kaggle competitions, where we demonstrate how a different SOTA candidate than the observed maximum can be estimated, and how it impacts the perceived results.

This work shows that for some cases, an unbiased SOTA estimate can be calculated fairly easily through bootstrapping, and can serve as a better reference point when introducing new methods to the scientific community. In other cases, the SOTA estimation is more complicated.

References

John W Tukey. The philosophy of multiple comparisons. *Statistical Science*, 6: 100–116, 1991. URL https://www.jstor.org/stable/2245714#metadata_info_tab_contents.

- Craig M Bennett, Abigail A Baird, Michael B Miller, and George L Wolford. Neural correlates of interspecies perspective taking in the post-mortem atlantic salmon: An argument for multiple comparisons correction. *Neuroimage*, 47:S125, 2009.
- Janez Demšar. Statistical comparisons of classifiers over multiple data sets. *Journal of Machine Learning Research*, 7:1–30, 2006.
- Steven L. Salzberg. On comparing classifiers: Pitfalls to avoid and a recommended approach. *Data Mining and Knowledge Discovery*, 1:317–328, 1997. ISSN 13845810. doi: 10.1023/A:1009752403260/METRICS. URL <https://link.springer.com/article/10.1023/A:1009752403260>.
- William Hedley Thompson, Jessey Wright, Patrick G. Bissett, and Russell A. Poldrack. Dataset decay and the problem of sequential analyses on open datasets. *eLife*, 9:1–17, 5 2020. ISSN 2050084X. doi: 10.7554/ELIFE.53498.
- Damien Teney, Ehsan Abbasnejad, Kushal Kafle, Robik Shrestha, Christopher Kanan, and Anton van den Hengel. On the value of out-of-distribution testing: An example of goodhart’s law. *Advances in Neural Information Processing Systems*, 33:407–417, 2020.
- Antonio Torralba and Alexei A. Efros. Unbiased look at dataset bias. *Proceedings of the IEEE Computer Society Conference on Computer Vision and Pattern Recognition*, pages 1521–1528, 2011. ISSN 10636919. doi: 10.1109/CVPR.2011.5995347.
- Mark Everingham, S. M.Ali Eslami, Luc Van Gool, Christopher K.I. Williams, John Winn, and Andrew Zisserman. The pascal visual object classes challenge: A retrospective. *International Journal of Computer Vision*, 111:98–136, 1 2015. ISSN 15731405. doi: 10.1007/S11263-014-0733-5/FIGURES/27. URL <https://link.springer.com/article/10.1007/s11263-014-0733-5>.
- Manuel Fernández-Delgado, Eva Cernadas, Senén Barro, Dinani Amorim, and Amorim Fernández-Delgado. Do we need hundreds of classifiers to solve real world classification problems? *Journal of Machine Learning Research*, 15:3133–3181, 2014. URL <http://www.mathworks.es/products/neural-network>.
- Avrim Blum and Moritz Hardt. The ladder: A reliable leaderboard for machine learning competitions. pages 1006–1014. PMLR, 6 2015. URL <https://proceedings.mlr.press/v37/blum15.html>.
- Cynthia Dwork, Vitaly Feldman, Moritz Hardt, Toniann Pitassi, Omer Reingold, and Aaron Roth. Guilt-free data reuse. *Communications of the ACM*, 60:86–93, 4 2017. ISSN 15577317. doi: 10.1145/3051088.

- Benjamin Recht, Rebecca Roelofs, Ludwig Schmidt, and Vaishaal Shankar. Do imagenet classifiers generalize to imagenet? pages 5389–5400. PMLR, 5 2019. URL <https://proceedings.mlr.press/v97/recht19a.html>.
- Vitaly Feldman, Roy Frostig, and Moritz Hardt. The advantages of multiple classes for reducing overfitting from test set reuse. pages 1892–1900. PMLR, 5 2019. URL <https://proceedings.mlr.press/v97/feldman19a.html>.
- Horia Mania, John Miller, Ludwig Schmidt, Moritz Hardt, and Benjamin Recht. Model similarity mitigates test set overuse. *Advances in Neural Information Processing Systems*, 32, 2019.
- Rebecca Roelofs, Vaishaal Shankar, Benjamin Recht, Sara Fridovich-Keil, Moritz Hardt, John Miller, and Ludwig Schmidt. A meta-analysis of overfitting in machine learning. *Advances in Neural Information Processing Systems*, 32, 2019. URL <https://www.kaggle.com/kaggle/meta-kaggle>.
- Thomas G. Dietterich. Approximate statistical tests for comparing supervised classification learning algorithms. *Neural Computation*, 10:1895–1923, 10 1998. ISSN 0899-7667. doi: 10.1162/089976698300017197. URL <https://direct.mit.edu/neco/article/10/7/1895/6224/Approximate-Statistical-Tests-for-Comparing>.
- Odd Erik Gundersen and Sigbjørn Kjensmo. State of the art: Reproducibility in artificial intelligence. *Proceedings of the AAAI Conference on Artificial Intelligence*, 32:1644–1651, 4 2018. ISSN 2374-3468. doi: 10.1609/AAAI.V32I1.11503. URL <https://ojs.aaai.org/index.php/AAAI/article/view/11503>.
- Zhiyi Ma, Kawin, Ethayarajh, Tristan Thrush, Somya Jain, Ledell Wu, Robin Jia, Christopher Potts, Adina Williams, and Douwe Kiela. Dynaboard: An evaluation-as-a-service platform for holistic next-generation benchmarking. *Advances in Neural Information Processing Systems*, 34:10351–10367, 12 2021. URL <https://eval.ai>.
- Xavier Bouthillier, Pierre Delaunay, Mirko Bronzi, Assya Trofimov, Brennan Nichyporuk, Justin Szeto, Nazanin Mohammadi Sepahvand, Edward Raff, Kanika Madan, Vikram Voleti, Samira Ebrahimi Kahou, Vincent Michalski, Tal Arbel, Chris Pal, Gael Varoquaux, and Pascal Vincent. Accounting for variance in machine learning benchmarks. *Proceedings of Machine Learning and Systems*, 3:747–769, 3 2021.
- Olivier Bousquet and André Elisseeff. Stability and generalization. *Journal of Machine Learning Research*, 2:499–526, 2002. URL <http://sensitivity-analysis.jrc.cec.eu.int/>.
- Michel Talagrand. A new look at independence. *The Annals of Probability*, 24:1–34, 1996. URL https://www.jstor.org/stable/2244830#metadata_info_tab_contents.

- Gaël Varoquaux and Veronika Cheplygina. Machine learning for medical imaging: methodological failures and recommendations for the future. *npj Digital Medicine* 2022 5:1, 5:1–8, 4 2022. ISSN 2398-6352. doi: 10.1038/s41746-022-00592-y. URL <https://www.nature.com/articles/s41746-022-00592-y>.
- Philip J. Boland, Frank Proschan, and Y. L. Tong. Modelling dependence in simple and indirect majority systems. *Journal of Applied Probability*, 26:81–88, 3 1989. ISSN 0021-9002. doi: 10.2307/3214318. URL <https://www.cambridge.org/core/journals/journal-of-applied-probability/article/abs/modelling-dependence-in-simple-and-indirect-majority-systems/070D6335BDDDDC7AF4D70BC9B21B0B7B>.
- Daniel W. Ladd. An algorithm for the binomial distribution with dependent trials. *Journal of the American Statistical Association*, 70:333–340, 1975. ISSN 1537274X. doi: 10.1080/01621459.1975.10479867.
- Masato Hisakado, Kenji Kitsukawa, and Shintaro Mori. Correlated binomial models and correlation structures. 2006.
- Veronica Rotemberg, Nicholas Kurtansky, Brigid Betz-Stablein, Liam Caffery, Emmanouil Chousakos, Noel Codella, Marc Combalia, Stephen Dusza, Pascale Guitera, David Gutman, Allan Halpern, Brian Helba, Harald Kitzler, Kivanc Kose, Steve Langer, Konstantinos Lioprys, Josep Malvehy, Shenara Musthaq, Jabpani Nanda, Ofer Reiter, George Shih, Alexander Stratigos, Philipp Tschandl, Jochen Weber, and H. Peter Soyer. A patient-centric dataset of images and metadata for identifying melanomas using clinical context. *Scientific Data* 2021 8:1, 8:1–8, 1 2021. ISSN 2052-4463. doi: 10.1038/s41597-021-00815-z. URL <https://www.nature.com/articles/s41597-021-00815-z>.
- Martin J. Willemink, Wojciech A. Koszek, Cailin Hardell, Jie Wu, Dominik Fleischmann, Hugh Harvey, Les R. Folio, Ronald M. Summers, Daniel L. Rubin, and Matthew P. Lungren. Preparing medical imaging data for machine learning. *Radiology*, 295:4–15, 2 2020. ISSN 15271315. doi: 10.1148/RADIOL.2020192224/ASSET/IMAGES/LARGE/RADIOL.2020192224.FIG5B.JPEG. URL <https://pubs.rsna.org/doi/10.1148/radiol.2020192224>.
- Qishen Ha, Bo Liu, and Fuxu Liu. 10 2020. doi: 10.48550/arxiv.2010.05351. URL <https://arxiv.org/abs/2010.05351v1>.
- Fabio Mendoza Palechor and Alexis de la Hoz Manotas. Obesity or cvd risk (classify/regressor/cluster), 2023. URL <https://www.kaggle.com/dsv/7009925>.
- J A Hanley and B J McNeil. The meaning and use of the area under a receiver operating characteristic (roc) curve. *Radiology*, 143(1):29–36, Apr 1982. ISSN 0033-8419 (Print); 0033-8419 (Linking). doi: 10.1148/radiology.143.1.7063747.